Entanglement from a nanomechanical resonator weakly coupled to a single Cooper-pair box

L. Tian
Institute for Theoretical Physics, University of Innsbruck, 6020 Innsbruck, Austria;
Institut für Theoretische Festkörperphysik, Universität Karlsruhe, D-76128 Karlsruhe, Germany;
and Institute for Quantum Optics and Quantum Information of the Austrian Academy of Sciences, 6020 Innsbruck, Austria
(Received 29 August 2005; published 10 November 2005)

We present a quantum optics scheme of generating large-amplitude Schrödinger cat states and entanglement in a weakly coupled nanomechanical resonator and single Cooper-pair box system. We show that the entanglement in this system can be detected by a spectroscopic method and can be generated at finite temperature and in the presence of environmental fluctuations.

DOI: 10.1103/PhysRevB.72.195411 PACS number(s): 85.85.+j, 42.50.Vk, 85.25.Cp

I. INTRODUCTION

The fabrication and probing of ultrasmall nanomechanical resonators with secular frequencies of GHz and quality factors approaching 10^5 have been achieved in recent experiments.[1] These resonators are promising systems for demonstrating the quantum mechanical nature of the mechanical degrees of freedom.[2] One crucial step in studying the nanomechanical systems will be the engineering and detection of the quantum effects of the mechanical modes. This can be achieved by connecting the resonators with solid-state electronic devices,[1,3–5] such as a single-electron transistor (SET). The SET couples with the resonator via electrostatic interaction and measures the flexural oscillation of the resonator with an accuracy approaching the quantum limit.[1] Preparing a resonator to a pure state—e.g., its ground state—has been proposed using quantum feedback control via a SET (Ref. 6) and sideband cooling via a quantum dot (Ref. 7) or a single Cooper-pair box (SCPB) (Ref. 8).

Quantum engineering of the resonator modes, which are underdamped harmonic oscillators, can be achieved by applying the techniques in quantum optics. For example, connecting a resonator with a solid-state qubit forms a spin-oscillator model that has been intensively studied in quantum optics, especially in ion trap quantum computing.[9] The techniques of manipulating the motional state of a trapped ion by laser pulses can be applied to studying the nanomechanical resonators. One such system contains a nanomechanical resonator capacitively coupled with a SCPB which acts as a quantum two-level system—the superconducting charge qubit—controlled by the gate voltage.[10] In Refs. 3–5, this system was studied and it was shown that entanglement between the resonator and qubit can be generated and detected by interferometry when the coupling is *stronger* than the frequency of the resonator. However, in experiments the coupling is usually small, limited by both the geometry between the charge island and the resonator and the maximal voltage that can be applied[8] and *cannot* meet the above condition.

In this paper, we present an approach that generates large-amplitude Schrödinger cat states and entanglement in this system even at *small* coupling by parametric pumping of the SCPB. Given the large amplitude of the generated states, the entanglement between the resonator and qubit can be observed spectroscopically. When generalized to two or more nanomechanical resonators, this scheme generates entanglement between these resonators which has potential applications in the detection of weak forces, precision measurement, and quantum information processing.[11–13] The effects of nonideal pulses, noise, and finite temperature on this scheme are also discussed. Moreover, this scheme can be generalized to other systems involving generic spin-oscillator coupling. As an example, we show that measurement of the states of an electron spin[14,15] can be achieved in the magnetic resonance force microscopy (MRFM) system. This paper is organized as follows. In Sec. II, we present the coupling between a nanomechanical resonator and a SCPB in a rotating frame. In Sec. III, we describe the parametric scheme that amplifies the displacement of the resonator by pumping the charge qubit. A detection scheme is then presented in Sec. IV, where a spectroscopic approach is studied to detect the entanglement in the system. In Sec. V, we study the effects of nonideal situations on the realization of our scheme, including nonideal pulses, environmental fluctuations, and finite temperature. A generalization of this scheme to another spin-oscillator system—detection of the states of single spin—is studied in Sec. VI. Finally, we conclude in Sec. VII.

II. THE SYSTEM

The coupled system of a nanomechanical resonator and a SCPB is shown in Fig. 1(a), with the resonator undergoing flexural vibration. The flexural mode is described by the Hamiltonian $H_m=\hbar\omega_0\hat{a}^\dagger\hat{a}$ with ω_0 the frequency and $\hat{a}^\dagger$ ($\hat{a}$) the raising (lowering) operator of the mode. The resonator is biased at a voltage $V_x(t)$ and couples to the SCPB through a capacitance $C_x(\hat{x})=C_{x0}(1+\hat{x}/d_0)$ where C_{x0} is the static capacitance, d_0 the static distance between the resonator and the qubit, and $\hat{x}=\delta x_0(\hat{a}+\hat{a}^\dagger)$ the displacement of the flexural mode with $\delta x_0=\sqrt{\hbar/2m\omega_0}$. The SCPB is a superconducting island connected with Josephson junctions and is controlled by the phase $\phi_x(t)$ and gate voltage $V_g(t)$ via the gate capacitance C_g. When $C_gV_g+C_{x0}V_x\sim e(2n+1)+2e\delta n$ with n integer and δn small, the SCPB can be treated as an effective quantum two-level system—the superconducting charge qubit[10,16]—described by the Hamiltonian $H_q=4E_c\delta n\sigma_z+[E_J(t)/2]\sigma_x$ with $E_J(t)$ the Josephson energy, $E_c=e^2/2C_\Sigma$

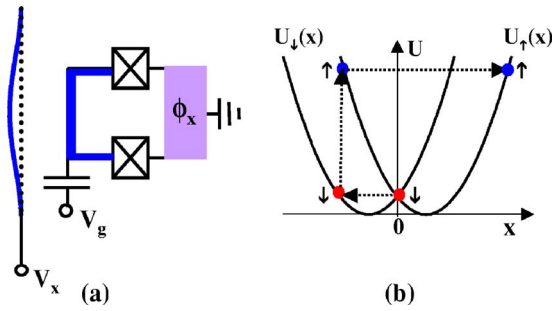

FIG. 1. (Color online) (a) The coupled system. The SCPB is made of two Josephson junctions and biased by the gate voltage V_g. The phase ϕ_x controls the Josephsen energy of the SCPB. The resonator is biased at the voltage V_x. (b) The evolution of the resonator starting from $x=0$ and $|\downarrow\rangle$. The parabolic curves are the qubit-dependent harmonic potentials $U_{\uparrow,\downarrow}(x)$. The solid circles indicate the position and energy of the resonator with the qubit state labeled as $\uparrow,\downarrow$. The dotted arrows describe the displacement and the increase in energy of the resonator.

the charging energy, and C_Σ the total capacitance connecting to the charge island. Here $\sigma_{x,z}$ are Pauli operators for the two-level system. The Josephson energy includes a static part E_{J0} and a small ac part adjusted by the phase $\phi_x(t)$ which can be controlled by external flux or bias current.[16] To the lowest order, the coupling between the resonator and SCPB is $-\lambda(t)(\hat{a}+\hat{a}^\dagger)\sigma_z$ where $\lambda(t)=(2E_c/e)V_x(t)C_{x0}\,\delta x_0/d_0$ with its magnitude limited by the small ratio $\delta x_0/d_0$ and the applied voltage V_x. In our scheme, the resonator is biased with an ac voltage $V_x(t)=V_{x0}\cos(\omega_{ac}t)$ with amplitude V_{x0} and frequency ω_{ac}, and the gate voltage is $V_g(t)=V_{dc}+V_{g0}\cos(\omega_{ac}t)$, including a dc part V_{dc} with $C_gV_{dc}=e(2n+1)$ and an ac part with amplitude V_{g0} and the same frequency ω_{ac}. The driving frequency satisfies $\omega_{ac}=E_{J0}/\hbar$. In the following we study the system in the rotating frame of $(E_{J0}/2)\sigma_x$, where the Hamiltonian in the rotating-wave approximation can be derived as

$$H_{rot}=\hbar\omega_0\hat{a}^\dagger\hat{a}-\frac{\lambda_0}{2}(\hat{a}+\hat{a}^\dagger)\sigma_z-\frac{\epsilon_z}{2}\sigma_z+\frac{\epsilon_\perp(t)}{2}\sigma_x, \qquad (1)$$

where the coupling is

$$\lambda_0=4E_c\frac{V_{x0}C_{x0}}{2e}\frac{\delta x_0}{d_0},$$

$$\epsilon_z=\frac{4E_c}{e}(C_gV_{g0}+C_{x0}V_{x0})\ll E_c,$$

and $\epsilon_\perp$ is the small ac modulation of E_{J0}. Hence the dynamics of the resonator is that of a shifted harmonic oscillator with the Hamiltonian $D_0(\sigma_z)H_mD_0^\dagger(\sigma_z)$ with

$$D_0(\sigma_z)=\exp\left(-(\hat{a}-\hat{a}^\dagger)\frac{\lambda_0\sigma_z}{2\hbar\omega_0}\right)$$

being the displacement operator. Typical parameters[8] are $E_{J0}\approx 10$ GHz, $E_c\approx 50$ GHz, $C_{x0}\approx 20$ aF, and $\omega_0\approx 100$ MHz. At $V_{x0}\approx 1$ V, the coupling is $\lambda_0\approx 20$ MHz.

III. AMPLIFICATION SCHEME

Below we show that by pumping the charge qubit with stroboscopic pulses, large-amplitude Schrödinger cat states and entanglement can be generated in this system. In an ideal situation, we consider δ-function pulse sequence

$$\epsilon_\perp(t)=\pi\sum_n\delta(n\tau_0), \quad \text{with } n\geqslant 1, \quad \text{integer}, \qquad (2)$$

where each pulse generates a transformation $-i\sigma_x$ that flips the charge qubit every half period $\tau_0=\pi/\omega_0$ of the resonator. Here we assume zero charge bias $\epsilon_z=0$—i.e., working at the degenerate point with a long coherence time.[16] The δ-function approximation is valid when $\epsilon_\perp\gg\hbar\omega_0,\lambda_0$. Let U_1 be the free evolution between the pulses. We have $U_1=D_0(\sigma_z)e^{-i\pi\hat{a}^\dagger\hat{a}}D_0^\dagger(\sigma_z)$. After the nth pulse, the unitary transformation on the system is $U(n\tau_0)=(-i\sigma_xU_1)^n$. With the relations $\sigma_xD_0(\sigma_z)\sigma_x=D_0^\dagger(\sigma_z)$ and $e^{i\pi\hat{a}^\dagger\hat{a}}D_0(\sigma_z)e^{-i\pi\hat{a}^\dagger\hat{a}}=D_0^\dagger(\sigma_z)$, we derive

$$U(n\tau_0)=\begin{cases}D_0^{2n}(-\sigma_z), & n\in\text{even},\\ \sigma_xe^{-i\pi\hat{a}^\dagger\hat{a}}D_0^{2n}(-\sigma_z), & n\in\text{odd},\end{cases} \qquad (3)$$

with the overall phase factors omitted. This transformation generates on the resonator a spin-dependent displacement $\Delta x=-\delta x_0(2n\lambda_0\sigma_z/\hbar\omega_0)$ when n is even and an opposite displacement when n is odd. Hence entanglement can be generated between the qubit and the resonator.[9]

Assume an initial state $(1/\sqrt{2})(|\uparrow\rangle+|\downarrow\rangle)|0\rangle$ where $|0\rangle$ is the ground state of the resonator and $|\uparrow,\downarrow\rangle$ are eigenstates of the charge qubit in the σ_z basis. After even number of pulses n, the state $(1/\sqrt{2})(|\uparrow\rangle|-2n\alpha_0\rangle+|\downarrow\rangle|2n\alpha_0\rangle)$ is generated where $\alpha_0=\lambda_0/2\hbar\omega_0$. The notation $|\alpha\rangle$ denotes a coherent state of the resonator with amplitude α. When $2n\alpha_0\gg 1$, maximal entanglement is generated between the resonator and charge qubit. This scheme can be applied to an arbitrary initial state of the resonator. An intuitive way of understanding the process is to consider a classical particle with two spin components in a harmonic potential that is shifted from the origin to the left (right) at spin down (up). The spin is subject to flips every half period of the oscillator, as shown in Fig. 1(b). The oscillator starts from the origin with spin down and oscillates to $x<0$ until the next flip. Each flip changes the spin component and increases the energy of the particle. Note that with the Hamiltonian in Eq. (1), entanglement can be generated between $|\uparrow\rangle|\alpha_0\rangle$ and $|\downarrow\rangle|-\alpha_0\rangle$ without the pulses.[4,5] However, in realistic situations $\lambda_0<\hbar\omega_0$, the coupling only slightly shifts the resonator state and the resonator is only weakly entangled with the charge qubit. With our pumping process, an amplitude much larger than α_0 can be achieved even at weak coupling.

Writing the generated state in the $|\pm\rangle$ basis with $|\pm\rangle=1/\sqrt{2}(|\uparrow\rangle+|\downarrow\rangle)$, we have $1/2|+\rangle(|-2n\alpha_0\rangle+|2n\alpha_0\rangle)+1/2|-\rangle(|-2n\alpha_0\rangle-|2n\alpha_0\rangle)$. A measurement on σ_x of the qubit[16] projects the resonator to the Schödinger cat states $(1/\sqrt{2})(|-2n\alpha_0\rangle\pm|2n\alpha_0\rangle)$ corresponding to the measured σ_x value $\pm$. When generalized to multiple resonators and (or) charge qubits, entanglement between the resonator modes can be generated. As an example, when two resonators couple with one

charge qubit with the coupling $\Sigma(\lambda_{0i}/2)(\hat{a}_i+\hat{a}_i^\dagger)\sigma_z$, the state $(1/\sqrt{2})(|-\alpha_1\rangle_1|-\alpha_2\rangle_2 \pm |\alpha_1\rangle_1|\alpha_2\rangle_2)$ can be generated after the flipping pulses. The index $i=1,2$ labels the two resonators and $\alpha_i=n\lambda_i/\hbar\omega_0$. Such states are maximally entangled states of the resonators[17] and are crucial elements in continuous variable quantum computing.[18] In addition, using N entangled resonators for weak force detection, the sensitivity can be improved by a factor of $\sqrt{N}$ compared with that of N independent resonators.[12]

IV. DETECTION OF ENTANGLEMENT

The entanglement between the resonator and charge qubit can be detected by a spectroscopic method when the amplitude of the resonator satisfies: $2n\alpha_0 \gg 1$. Below we study the detection of the state $(1/\sqrt{2})(|\uparrow\rangle|-2n\alpha_0\rangle+|\downarrow\rangle|2n\alpha_0\rangle)$. Here we divide the detection into two steps: the detection of the correlation between the resonator and charge qubit and the detection of the coherence between the spin-up part $|\uparrow\rangle|-2n\alpha_0\rangle$ and the spin-down part $|\downarrow\rangle|2n\alpha_0\rangle$).

In the first step, a static bias $\epsilon_z > 0$ on the charge qubit is turned on and the Josephson energy is modulated with a frequency ω_d for a duration of π/ω_d as $\epsilon_d \cos(\omega_d t)\sigma_x$. Here instead of the δ-function pulses in Eq. (2), the magnitude of ϵ_d is comparable to $8n\alpha_0\lambda_0$ and ϵ_z, while much larger than ω_0. So the resonator can be treated as static during the detection process. This condition is crucial for the detection scheme, and nonideal situations are studied in the next section. The effective Hamiltonian of the SCPB is

$$H_q^{|\pm 2n\alpha_0\rangle} = -\frac{\epsilon_z \pm 4n\alpha_0\lambda_0}{2}\sigma_z + \epsilon_d \cos(\omega_d t)\sigma_x, \tag{4}$$

where the energy splitting of the charge qubit depends on the resonator states $|\pm 2n\alpha_0\rangle$: $E_+=\epsilon_z+4n\alpha_0\lambda_0$ for the state $|2n\alpha_0\rangle$ and $E_-=\epsilon_z-4n\alpha_0\lambda_0$ for the state $|-2n\alpha_0\rangle$. The frequency of the ac modulation is chosen to be $\hbar\omega_d=\epsilon_z-4n\alpha_0\lambda_0$ in resonance with E_-. Hence the pulse flips the charge qubit in $H_q^{|-2n\alpha_0\rangle}$, while not in $H_q^{|2n\alpha_0\rangle}$. This pulse is followed by a δ-function $\pi/2$ pulse that transforms the states of the charge qubit from $|\uparrow,\downarrow\rangle$ to $|+,-\rangle$. The final state is then

$$-\frac{i}{\sqrt{2}}|-\rangle|-2n\alpha_0\rangle + \frac{1}{\sqrt{2}}(c_\downarrow|-\rangle + c_\uparrow|+\rangle)|2n\alpha_0\rangle, \tag{5}$$

with $c_\uparrow=-i\sin(\pi\bar{\epsilon}_d/2\epsilon_d)(\epsilon_d/\bar{\epsilon}_d)$ and

$$c_\downarrow = \cos\left(\frac{\pi\bar{\epsilon}_d}{2\epsilon_d}\right) - i\sin\left(\frac{\pi\bar{\epsilon}_d}{2\epsilon_d}\right)\frac{8n\alpha_0\lambda_0}{\bar{\epsilon}_d},$$

where $\bar{\epsilon}_d=\sqrt{\epsilon_d^2+(8n\alpha_0\lambda_0)^2}$. For the state $|\downarrow\rangle|2n\alpha_0\rangle$, the off resonance with the magnitude $8n\alpha_0\lambda_0$ between ω_d and E_+ prevents the charge qubit from flipping. For the state $|\uparrow\rangle|-2n\alpha_0\rangle$, the charge qubit flips to the state $|\downarrow\rangle$. When $8n\lambda_0 \gg \epsilon_d$, this shows that $|c_\downarrow|\approx 1$ while $|c_\uparrow|\approx 0$. Note that the states $|\pm\rangle$ are of the rotating frame and in the laboratory frame the σ_x eigenstates are $|\pm\rangle_s=e^{\pm iE_J t/\hbar}|\pm\rangle$. A measurement on the σ_x operator of the charge qubit[16] gives the probabilities of the states $|\pm\rangle$ as $p_-=(1+|c_\downarrow|^2)/2\approx 1$ and $p_+=|c_\uparrow|^2/2 \approx 0$. When there is no correlation between the resonator and charge qubit, $|c_\downarrow|\sim 0$ and $p_\pm \approx 1/2$. The correlation between the resonator and charge qubit hence affects the probabilities $p_\pm$ and can be revealed from this detection scheme.

In the next step, the detection starts by applying a δ-function $\pi/2$ pulse to the state $(1/\sqrt{2})(|\uparrow\rangle|-2n\alpha_0\rangle + |\downarrow\rangle|2n\alpha_0\rangle)$, which is followed by n pulses in Eq. (2). Written in the $|\pm\rangle$ basis of the charge qubit, the state becomes $(1/2\sqrt{2})(|+\rangle|\psi_+\rangle+|-\rangle|\psi_-\rangle)$ with

$$|\psi_+\rangle = |-4n\alpha_0\rangle + 2|0\rangle - |4n\alpha_0\rangle,$$

$$|\psi_-\rangle = |-4n\alpha_0\rangle + |4n\alpha_0\rangle, \tag{6}$$

as the wave functions of the resonator. The probabilities of the charge qubit on the states $|\pm\rangle$ are $p_+=3/4$ and $p_-=1/4$, respectively. While without the coherence—i.e., for a mixed state of $|\uparrow\rangle|-2n\alpha_0\rangle$ and $|\downarrow\rangle|2n\alpha_0\rangle$—$p_\pm=1/2$ after the pulses. Hence by measuring the charge qubit in the $|\pm\rangle$ basis, it can be shown that the system is in coherent superposition between the states $|\uparrow\rangle|-2n\alpha_0\rangle$ and $|\downarrow\rangle|2n\alpha_0\rangle$. Combining the above two steps, the entanglement between the resonator and qubit can be demonstrated. This detection scheme only requires measurement of the charge qubits and rf pulses that can be applied to the charge qubit.

V. NONIDEAL PULSES, NOISE, AND FINITE TEMPERATURE

In the above discussion, we assume ideal situations where the noise is neglected, temperature is zero, and the energy scales are well separated—i.e., $\epsilon_\perp \gg 8n\alpha_0\lambda_0$, ω_0 during the amplification and ϵ_z, ϵ_d, $8n\alpha_0\lambda_0 \gg \omega_0$ during the detection. Below we study the effect of these nonideal factors on the amplification and the detection schemes and show that entanglement can be generated in these nonideal situations.

The amplitudes of the pulses $\epsilon_\perp$, ϵ_d are limited by various energy scales in the system: the Josephson energy E_{J0}, the resonator frequency, and the coupling. Typical parameters are $E_{J0}=20$ GHz, $\omega_0=100$ MHz, and $\lambda_0=20$ MHz. We numerically simulate the amplification and the detection schemes with these parameters. The fidelity of the amplification process is calculated as $f(\epsilon_\perp)=|\langle\psi_{id}(t)|\psi(t)\rangle|^2$, where $|\psi_{id}\rangle$ is the target wave function by the ideal pulses and $|\psi(t)\rangle$ is the wave function by pulses of the above parameters, as is shown in Fig. 2. It can be seen that at $\epsilon_\perp=10\omega_0$, the fidelity is very low with $f=0.7$ after $n=12$ pulses. However, the fidelity increases significantly with increasing $\epsilon_\perp$. At $\epsilon_\perp=60\omega_0$, corresponding to $\epsilon_\perp=6$ GHz, the fidelity is $f>0.99$ after $n=12$ pulses. We also simulate the detection process at various static bias ϵ_z and $\epsilon_d \in (0.5\omega_0, 10.5\omega_0)$. After $n=12$ pulses, $8n\alpha_0\lambda_0 \approx 1.9\omega_0$. In the inset of Fig. 2, p_- is plotted versus ϵ_d at $\epsilon_z=3.2\omega_0$ and $\epsilon_z=4.0\omega_0$. At $\epsilon_z=4.0\omega_0$, a maximum of p_- appears at $\epsilon_d=1.9\omega_0$ with $p_-=0.80$, very different from that of the mixed state. This shows that the entanglement can be generated and detected with the given parameters.

Another factor is the environmental noise which can affect the coherence of the system and hence the realization of the scheme. With given parameters $\alpha_0=0.1$ and $n>20$ flips,

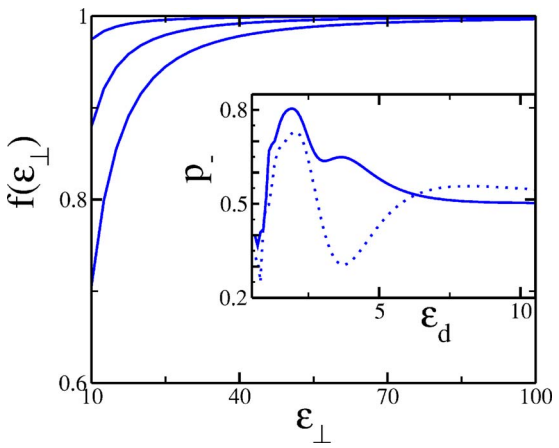

FIG. 2. (Color online) Main plot: the fidelity of the amplification versus $\epsilon_\perp$. The curves from top to bottom are for $n=4,8,12$ pulses. Inset: the probability p_- after the detection pulses versus ϵ_d at $\epsilon_z=4.0\omega_0$ (solid line) and $\epsilon_z=3.2\omega_0$ (dotted line). The axes of $\epsilon_{\perp,d}$ are in units of ω_0.

a duration of 100 nsec are required to have $2n\alpha_0 \gg 1$. It is crucial to have the decoherence time longer than this duration to successfully generate the entanglement between the resonator and SCPB. One source of decoherence is the charge noise of the qubit, dominated by the low-frequency charge fluctuations.[10] In our scheme, the qubit is operated at the degenerate point where a decoherence time as long as microseconds[16] has been observed. In the rotating frame of Eq. (1), this can be explained as a spectral shift that screens the low-frequency noise: in this frame the noise spectrum is $S^0(\omega \pm E_{J0}/\hbar)$ shifted from the spectrum $S^0(\omega)$ in the laboratory frame by E_{J0}. The low-frequency noise is screened by the Josephson energy and only has a higher-order effect on the qubit. Another source of decoherence is the mechanical noise of the resonator which is characterized by the quality factor Q. The decoherence rate is $\tau_{dec}^{-1}=(2\langle n\rangle+1)\omega_0/Q$ with n the average phonon number.[20] At temperature T, we have

$$\tau_{dec}^{-1} \approx \begin{cases} \dfrac{8(n\alpha_0)^2\hbar\omega_0}{Q}, & 2n\alpha_0 > \sqrt{\dfrac{k_BT}{\hbar\omega_0}}, \\ \dfrac{2k_BT}{Q}, & 2n\alpha_0 \leqslant \sqrt{\dfrac{k_BT}{\hbar\omega_0}}. \end{cases} \tag{7}$$

With $n=20$, $T=20$ mK, and $Q=10^4$, we derive $\tau_{dec}\approx 3$ nsec, which allows coherence during the realization of our scheme.

At finite temperature T, the resonator mode is in a mixed state with the density matrix $\rho_\beta=\Sigma p_m|m\rangle\langle m|$ with $p_m=e^{-\beta m}(1-e^{-\beta})$, where $\beta=\hbar\omega_0/k_BT$. This thermal distribution broadens the distribution of the resonator in phase space and is another factor that may affect the generation of entanglement. After applying the pulses in Eq. (2), the density matrix becomes

$$\sum_m p_m(|\uparrow\rangle D+|\downarrow\rangle D^\dagger)|m\rangle\langle m|(D^\dagger\langle\uparrow|+D\langle\downarrow|), \tag{8}$$

where $D=D_0^{2n}(\downarrow)$ is the shift operator. It has been shown that the state in Eq. (8) is a nonseparable state[19] under the condition of $2n\alpha_0 \gg \sqrt{k_BT/\hbar\omega_0}$. Hence entanglement between the resonator and SCPB can still be generated at finite temperature. At the same time, the entanglement can be shown experimentally, with the detection scheme studied in the previous section. For $2n\alpha_0 \gg \sqrt{k_BT/\hbar\omega_0}$, the detection pulse flips the charge qubit selectively and prepares the SCPB to have probabilities $p_-\approx 1$ and $p_+\approx 0$, the same as for the pure state. And the pulse sequence for observing the coherence brings $p_+\approx 3/4$ and $p_-\approx 1/4$, also the same as for the pure state.

VI. DETECTION OF THE STATES OF SINGLE ELECTRON SPIN

As the above scheme involves a generic spin-oscillator model,[9] it can be generalized to other physical systems. Below, we show that this amplification scheme can be a useful approach in the detection of the quantum states of a single electron spin in the magnetic resonance force microscopy[14,15] system. In MRFM, the spins on or near a surface interact with the magnetic particle attached to a cantilever and can be detected by observing their influence on the cantilever.[15] It is a potentially promising technique for both spin manipulation and spin detection in quantum computing. In recent state-of-the-art experiments,[14] the presence of single electron spin has been detected by measuring the frequency shift of a cantilever due to its coupling with the spins.

Here we apply our amplification scheme to this system. We use the same notations as in Eq. (1). The cantilever couples along the z axis with an electron spin as $(\lambda_0/2)(\hat{a}+\hat{a}^\dagger)\sigma_z$, where the coupling $\lambda_0=2\mu_BG\delta x_0$ is decided by the local magnetic field gradient G and the quantum width of the cantilever δx_0. The dimensionless coupling magnitude can be derived as $\alpha_0=\mu_BG/2m\omega_0^2\delta x_0$. The bias ϵ_z of the spin in the z axis results from a total magnetic field including the field from the magnetic tip on the cantilever and an optional external field. The spin can be pulsed in the x axis by time-dependent rf pulses $\epsilon_x(t)$. In our scheme following the pulses described in Eq. (2), for a local spin-1/2 particle near the tip of the cantilever and after n spin flips, the cantilever is displaced by $\pm 4n\alpha_0\delta x_0$, corresponding to the two states of the spin. With the parameters in experiments,[14] $\omega_0=5.5$ kHz, $\delta x_0=1.3\times 10^{-13}$ m, and a magnetic field gradient as high as $G=2\times 10^5$ T/m, we have $\alpha_0=0.15$. After $n=5000$ flips, the distance between the two resonator states corresponding to the two spin states is $8n\alpha_0\delta x_0\approx 8\times 10^{-10}$ m. This distance is well within the resolution of optical interferometry, and the state of the spin can then be determined from the detection of the cantilever. In this scheme, it is necessary for the spin flips to be much faster than the period of the cantilever. Given the kHz frequency of the cantilever and magnetic resonance pulses of GHz, this can be easily realized. Hence, this scheme provides a measurement of the state of the spin by increasing the magnitude of the signal from the cantilever, which will be hard to resolve without the amplification.

To detect the state of the spin, the signal of the cantilever has to overcome the noise from environmental fluctuations. The displacement of the amplification is limited mainly by the dissipation of the cantilever and the spin correlation time. With a quality factor Q, the maximal displacement is

$\sim 8\alpha_0 \delta x_0 Q/\pi$, which corresponds to a maximal number of $n_{\max} \sim Q/\pi$ flips. The spin correlation time also limits the maximal number of flips. With $Q=5\times10^4$ and the measured correlation time on the order of 10 sec,[14] our scheme with $n=5000$ and a duration of ~ 0.5 sec can be realized. Meanwhile, the displacement is broadened at finite temperature with a width of $\delta x_0 \sqrt{k_B T/\hbar\omega_0}$ with $k_B T/\hbar\omega_0 \gg 1$. To resolve the spin states, it is required that $8n\alpha_0 \gg \sqrt{k_B T/\hbar\omega_0}$. At $T=1$ K, the broadening is 2×10^{-10} m and this condition is satisfied by the parameters above.

Hence a measurement of the electron spin states can be performed directly in the z basis with this scheme. While in the conventional cyclic adiabatic inversion technique[15] (CAI) widely used in MRFM, the spins are locked or antilocked with the local magnetic field in the rotating frame and adiabatically follow the rotation of the field. Furthermore, the displacement of the cantilever is significantly increased by applying parametric pulses to the spin, which results in the increase in the magnitude of the signal. This enables the signal to overcome environmental fluctuations[14] and the detection of the quantum state of single electron spin.

VII. CONCLUSION

We have studied a quantum optics scheme of generating and detecting Schrödinger cat states and entanglement in the weakly coupled resonator and SCPB system. By applying parametric pulses to the SCPB, amplification of the displacement of the nanomechanical resonator can be achieved and entanglement can be generated between the resonator and SCPB or between resonators. We also studied the effect of nonideal pulses by numerical simulation and analyzed the effects of environment and finite temperature on this scheme. In addition, we point out that this idea can be generalized to other systems. We studied the application of this scheme to the detection of the quantum state of single electron spin in the MRFM system.

ACKNOWLEDGMENTS

We thank I. Wilson-Rae, A. Shnirman, and P. Zoller for helpful discussions. This work is supported by the Austrian Science Foundation, the CFN of the DFG, the Institute for Quantum Information, and the EU IST Project SQUBIT.

[1] R. G. Knobel and A. N. Cleland, Nature (London) **424**, 291 (2003); M. D. LaHaye, O. Buu, B. Camarota, and K. C. Schwab, Science **304**, 74 (2004).

[2] A. N. Cleland and M. L. Roukes, Nature (London) **392**, 160 (1998); H. G. Craighead, Science **290**, 1532 (2000); X. Huang, C. A. Zorman, M. Mehregany, and M. L. Roukes, Nature (London) **421**, 496 (2003).

[3] M. Blencowe, Phys. Rep. **395**, 159 (2004).

[4] A. D. Armour, M. P. Blencowe, and K. C. Schwab, Phys. Rev. Lett. **88**, 148301 (2002).

[5] E. K. Irish and K. Schwab, Phys. Rev. B **68**, 155311 (2003).

[6] A. Hopkins, K. Jacobs, S. Habib, and K. Schwab, Phys. Rev. B **68**, 235328 (2003).

[7] I. Wilson-Rae, P. Zoller, and A. Imamoglu, Phys. Rev. Lett. **92**, 075507 (2004).

[8] I. Martin, A. Shnirman, L. Tian, and P. Zoller, Phys. Rev. B **69**, 125339 (2004).

[9] D. J. Wineland *et al.*, J. Res. Natl. Inst. Stand. Technol. **103**, 259 (1998).

[10] Y. Makhlin, G. Schön, and A. Shnirman, Rev. Mod. Phys. **73**, 357 (2001).

[11] V. B. Braginsky and F. Y. Khalili, *Quantum Measurement* (Cambridge University Press, Cambridge, England, 1992).

[12] W. J. Munro, K. Nemoto, G. J. Milburn, and S. L. Braunstein, Phys. Rev. A **66**, 023819 (2002).

[13] A. N. Cleland and M. R. Geller, Phys. Rev. Lett. **93**, 070501 (2004).

[14] D. Rugar, R. Budakian, H. J. Mamin, and B. W. Chui, Nature (London) **430**, 329 (2004); H. J. Mamin, R. Budakian, B. W. Chui, and D. Rugar, Phys. Rev. Lett. **91**, 207604 (2003).

[15] J. A. Sidles, J. L. Garbini, K. J. Bruland, D. Rugar, O. Züger, S. Hoen, and C. S. Yannoni, Rev. Mod. Phys. **67**, 249 (1995).

[16] D. Vion, A. Aassime, A. Cottet, P. Joyez, H. Pothier, C. Urbina, D. Esteve, and M. H. Devoret, Science **296**, 886 (2002).

[17] B. Kraus, K. Hammerer, G. Giedke, and J. I. Cirac, Phys. Rev. A **67**, 042314 (2003).

[18] S. Lloyd and S. L. Braunstein, Phys. Rev. Lett. **82**, 1784 (1999).

[19] S. Bose, I. Fuentes-Guridi, P. L. Knight, and V. Vedral, Phys. Rev. Lett. **87**, 050401 (2001).

[20] L. D. Landau and E. M. Lifshitz, *Statistical Physics* (Pergamon Press, New York, 1980).